A High-Isolation MIMO Antenna with Dual-Port Structure for 5G Mobile Phones

Hyung-kyu Yang[1], Won-Woo Lee[2], and Byung-Ho Rhee[3]*
[1] Electronic, Electrical, Control & Instrumentation Engineering, Hanyang University, Seoul, Rep. of Korea
[e-mail: sheep@kopo.ac.kr]
[2] ICT Convergence Research Division, Korea Expressway Corporation Research Institute, Gyeonggii-do, Rep. of Korea
[e-mail: wonwoo2.lee@gmail.com]
[3] The Division of Computer Science and Engineering, Hanyang University, Seoul, South Korea
[e-mail: bhrhee@hanyang.ac.kr]
*Corresponding author: Byung-Ho Rhee

Received April 16, 2017; revised August 10, 2017; revised October 17, 2017; accepted November 29, 2017; published April 30, 2018

Abstract

In this letter, a new dual-port Multiple-Input Multiple-Output (MIMO) antenna is introduced which has two independent signal feeding ports in a single antenna element to achieve smaller antenna volumes for the 5G mobile applications. The dual-port structure is implemented by adding a cross coupled semi-loop (CCSL) antenna as the secondary radiator to the ground short of inverted-F antenna (IFA). It is found that the port to port isolation is not deteriorated when an IFA and CCSL is combined to form a dual-port structure. The isolation property of the proposed antenna is compared with a polarization diversity based dual-port antenna proposed in the literature [9]. The operating frequency range is 3.3–4.0 GHz which is suitable for places where 4x4 MIMO systems are supposed to be deployed such as in China, EU, Korea and Japan at the band x (3.3 – 3.8GHz. The measured 6-dB impedance bandwidths of the proposed antennas are larger than 700 MHz with isolation between the feeding ports higher than 18 dB [1-2]. The simulation and measurement results show that the proposed antenna concept is a very promising alternative for 5G mobile applications.

Keywords: 5G, Antenna, coupled antenna, dual-port, ECC, loop antenna, LTE, MIMO, polarization diversity.

1. Introduction

The need of cellular frequency ranges below 6 GHz has been addressed in 5G mobile standardization groups [3-4] because of the insufficient available frequency bandwidth in the frequency bands below 3 GHz. One of the major use case of 5G service is to have a certain level of tight interworking with existing radio standards especially with long term evolution advanced Pro (LTE-A Pro) [4]. In such case, the demand for the number of supported antenna will be dramatically increased again because of LTE and LTE-A. Considering the higher order Multiple-Input Multiple Output (MIMO) operation and additional frequency bands to be defined below 6 GHz, 5G smartphones will have to support greater number of frequency bands than current 4G smartphones.

Furthermore, the additional receiving antennas are required for 4×4 MIMO support [5-6]. Therefore, it will be great challenges for device manufactures to integrate such a large number of antennas into smartphones with iconic designs. To overcome this problem, providing more than one signal port in a single antenna element can reduce the number of antenna, and therefore the smaller total antenna volume. Therefore, the dual-port antenna structure proposed in this paper can be an alternative solution for 4x4 MIMO antenna applications.

There have been several studies on dual-port antennas based on planar inverted F-shaped antennas (PIFA) in effort to reduce the total antenna volume [7-9]. These studies revealed that the port to port isolation was the main drawback of PIFA or IFA based dual-port antennas and several techniques have been proposed to improve the port to port isolation properties [7-8]. In [7], two feed ports are placed on 40x20 mm radiator plate in a perpendicular way to implement dual feed PIFA structure, and the isolation between the feed ports was achieved by reducing direct current flows at the ground plane between two feeding ports with etched ground structure. The authors further optimized the size in [8] but these two studies had drawbacks in realization of the real device form factors due to the size and the special requirement for ground plane shape. In [9], two PIFA are merged into a single unit to be orthogonally oriented toward each other to achieve better isolation. However, two PIFA with volumes of 23.5x10x7.5 mm and 35.6x5x5 mm have been used, which is relatively large size for mobile phones and therefore the advantage of using dual feed antenna structure could be limited.

In this letter, dual-port antenna design is proposed by merging IFA and a cross coupled semi-loop (CCSL) antenna. Therefore the space between the two antennas of the MIMO system is reduced and it has a more size efficient. A good isolation between the IFA branch and the CCSL branch can be achieved due to the fact that the resonance mode of IFA is transverse electric (TE) and that of CCSL is transverse magnetic (TM) mode and thereby the two resonance modes are orthogonal to each other. The operating frequency of the proposed antenna is at 3.5 GHz band. In recent years, 3.5 GHz bands are increasingly selected as 4x4 MIMO deployment as 3.5 GHz band has the widest available bandwidth and suitable for advanced antenna system such as massive MIMO technologies due to shorter wavelength.

We present contrasting performance results between the proposed dual-port antenna based on coupling pattern and the polarization diversity based dual-port antenna structure proposed in the literature [9].

2. Antenna Designs

Fig. 1 and **2** show the picture of prototypes and antenna layout schematics for the two types

of antenna designs to be compared in this letter. The proposed dual-port antenna based on CCSL antenna (type 1 going forward) is presented in **Fig. 1 (a)** and **2 (a)**. The polarization diversity based dual-port antenna (type 2) without CCSL in [9] is illustrated in **Fig. 1 (b)** and **2 (b)** as a reference antenna. The operating frequency ranges of the two prototype antennas are 3.3-4.0 GHz. The antennas are fabricated on the evaluation board with a size of 60 × 100 mm^2. The Printed Circuit Board (PCB) is made from FR4 with a relative permittivity (ε_r) of 4.4. For type 1 antenna, a coupled element is used as the secondary signal feed port (port 2) which forms semi-loop antenna with the inverted L-shaped branch from ground short. Primary signal feed port (port 1) is branched from the radiator like a normal IFA type of antenna. The feeding lines are designed in a way that the two feeding lines are perpendicular to each other to maximize the isolation between the two signal ports. For type 2 antenna, both of the signal ports are directly branched from each radiator. Notice that the two radiators are orthogonally oriented to each other for polarization diversity. To feed the antennas, SMA-connected 50-Ω coaxial cables are soldered on each port of the antennas. All measurements are taken using an RF choke in order to avoid efficiency contribution from currents flowing on the measurement cable [10].

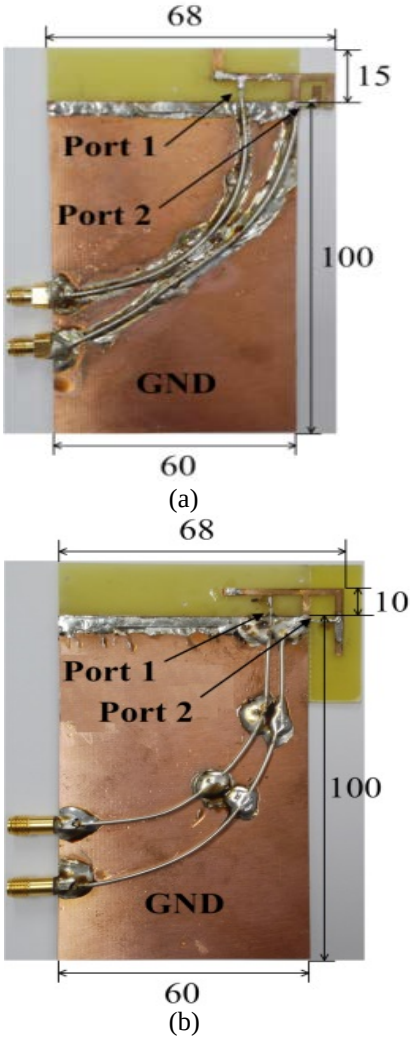

Fig. 1. Photography of fabricated antennas. (a) Type 1: Dual-port antenna based on CCSL antenna, (b) Type 2: Dual-port antenna based on polarization diversity proposed in [9]

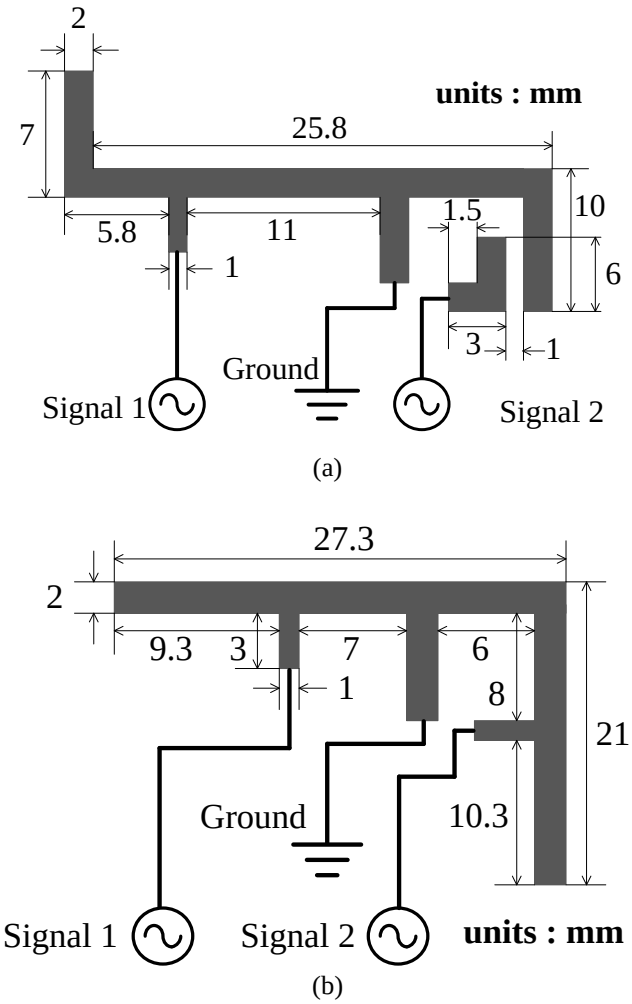

Fig. 2. Schematic designs of antennas, a) Type 1: Dual-port antenna based on CCSL antenna, (b) Type 2: Dual-port antenna based on polarization diversity.

3. Simulation Results

The simulated surface current distributions on ground plane and antenna at 3.5 GHz are illustrated in **Fig. 3** for the two types of antennas. For the simulation work and optimization of the geometric parameters of the antennas, we use Computer Simulation Technology (CST) (MICROWAVE STUDIO 2011) for this study [11]. The simulations are conducted by exiting port 2 to compare the current distribution characteristics between the two different types of antennas for how the current induced by the port 2 impacts on the current distributions near the port 1 and the associated antenna radiator. Port 1 (left antenna) and Port 2 (right antenna) are set as terminated with 50- resistors and excited, respectively. In this way we can compare the port to port isolation characteristics of the two types of antennas.

Fig. 3 (a) shows the current distributions for type 1 antenna. It is observed that the surface current at port 1 is not highly concentrated when port 2 is excited. This suggests that the contribution of port 1 to the radiation is small and therefore good port to port isolation

characteristics are expected. On the other hand, for the case of type 2 antenna as presented in **Fig. 3 (b)**, a large current density is observed in between the two signal ports due to port 2 excitation meaning that the port 1 contributes to radiation when port 2 is excited and this impacts on the isolation between the port 1 and port 2.

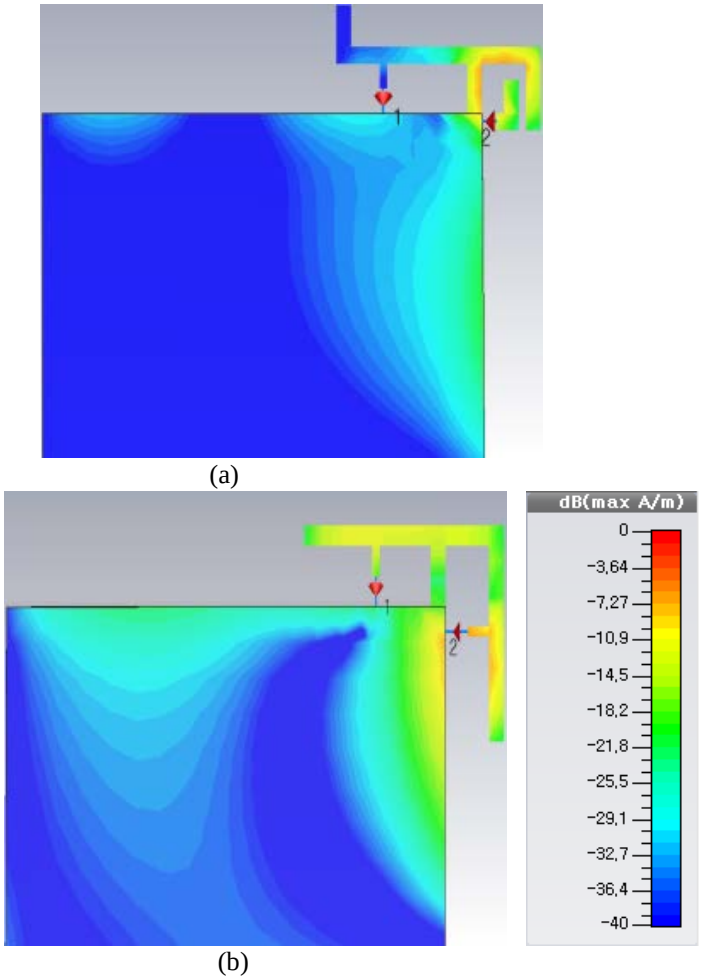

Fig. 3. Simulated current distributions at 3.5 GHz, a) Type 1: Dual-port antenna based on CCSL antenna, (b) Type 2: Dual-port antenna based on polarization diversity.

Fig. 4 shows the simulated current flow distributions on the ground plane of the antenna and on the radiating plate excited by the dual antenna. The current distributions for the primary signal port and for the secondary signal port are illustrated in **Fig. 4 (a)** and **Fig. 4 (b)**, respectively. It should be noted that the directions of the current flows created by each port of the dual antenna are clearly different each other. The current flow with high density area for the primary signal (port 1) is in the horizontal direction and it is concentrated in the top corner, whereas the current flow of high density area for the secondary signal (port 2) is in the vertical direction and it is concentrated in the right corner. Such a difference in the direction of the current flow between the two signal ports and separation for current flow with high density are the key aspect of ensuring good isolation between two ports.

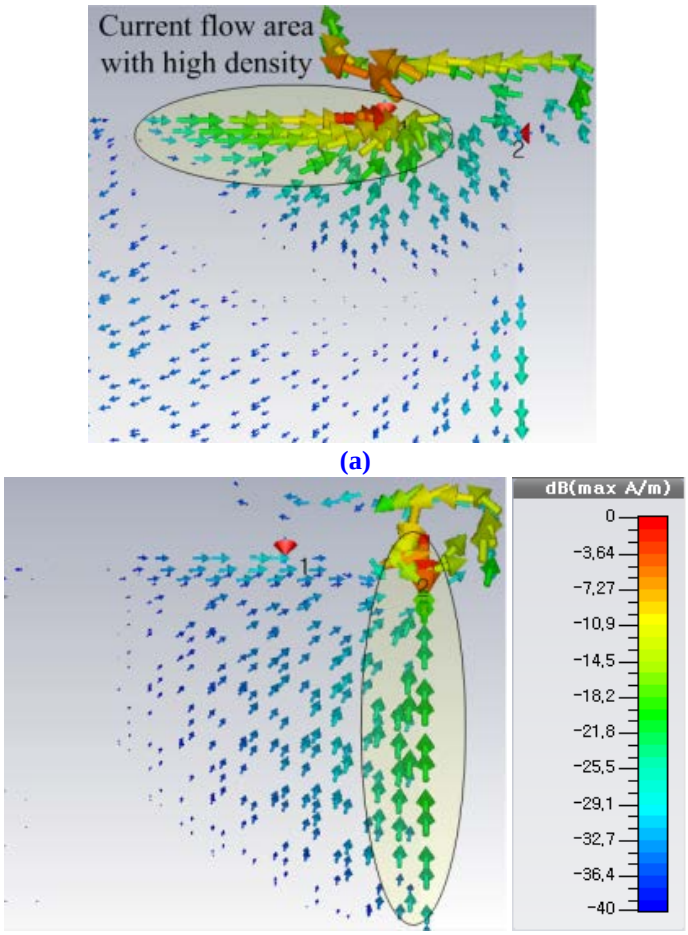

(a)

(b)

Fig. 4. Simulated current distributions at 3.5Ghz for Type 1, a) Current flow of primary signal (port 1), b) Current flow of secondary signal (port 2)

4. Measurement Results

Fig. 5 shows the simulated and measured frequency responses of the scattering parameters for the two types of antennas. Both of the antennas show well matched impedance characteristics over the antenna bandwidth. It is notable that the overall bandwidth of frequency responses for type 1 is much wider than those for type 2 antenna. This can be attributed to the cross coupled structure of CCSL. It is interesting to find that the port to port isolation property of type 1 antenna is almost flat and well below -18 dB over the antenna bandwidth. In case of type 2, it shows much narrower bandwidth of frequency responses than that of type 1, especially for the isolation. The simulation results tell that type 1 antenna shows approximately 8 dB better isolation at 3.5 GHz than type 2 antenna. The measurement results have a good agreement with the simulation results in general. The slight differences exist due to the effect of coherency and manufacturing tolerance by the influences of the feed cables and the misalignment of the antenna resonant frequency and the coupling null [12]. Both the simulation and measurement results confirm that type 1 antenna shows better port to port isolation characteristics than type 2 antenna and we believe that this result is significantly distinctive isolation performance in isolations of two independent co-located antennas.

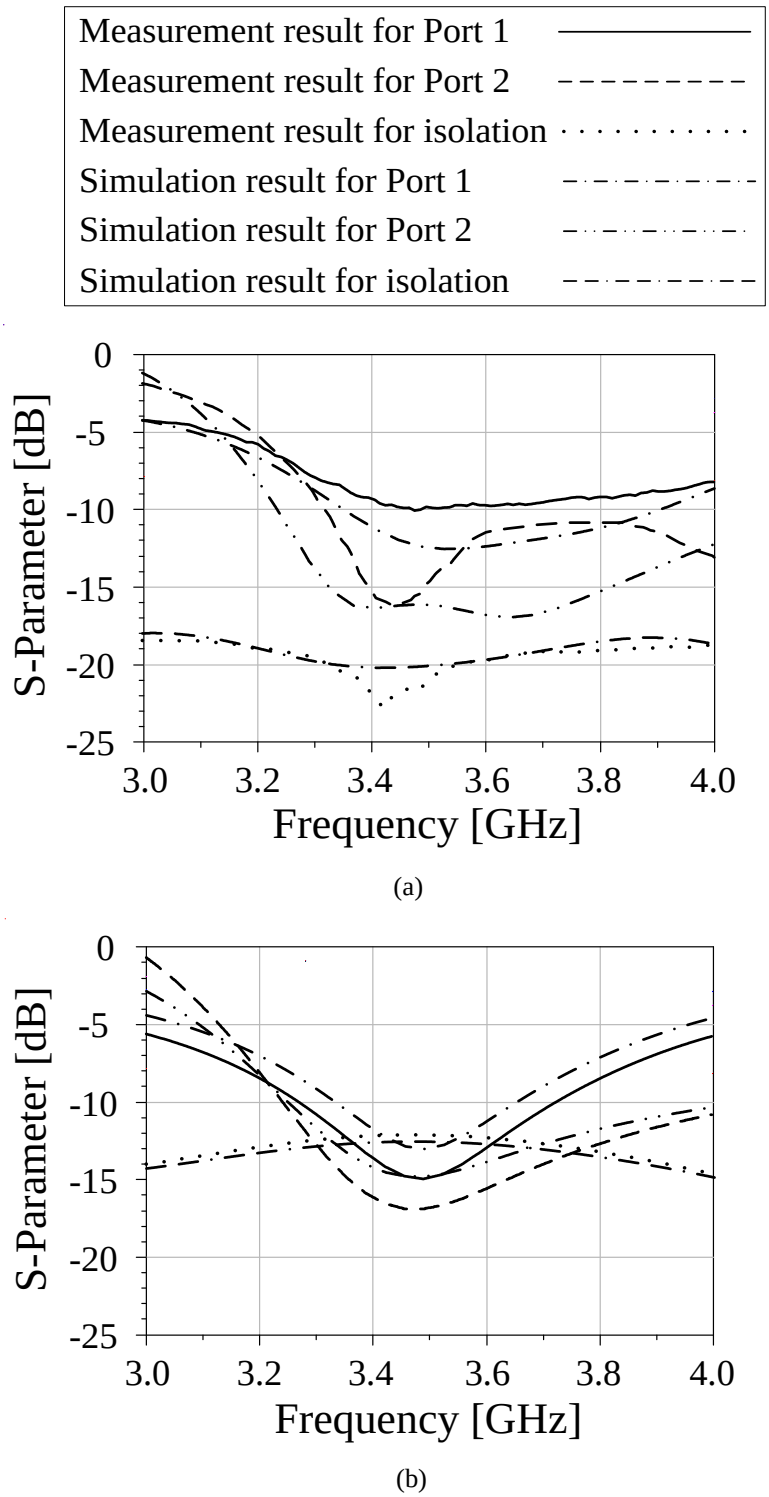

Fig. 5. Simulated and Measured S-parameter characteristics for the proposed antenna, a) Type 1: Dual-port antenna based on CCSL antenna, (b) Type 2: Dual-port antenna based on polarization diversity

Fig. 6 shows the measured average gain over the operating bandwidth of the two types of antennas. The gain measurements of the antennas are executed by using Microwave Technologies Group version 2.1 (MTG ver.2.1), a 3D measurement system [13]. **Fig. 6** shows the measured average gain over the operating BW of the proposed antenna system. The measured average gain for the primary signal of type1, is approximately -2.05 dBi to -0.34 dBi with the gain variation of 1.71 dB. For the secondary antenna, the average gain is from -1.81 dBi to -0.16 dBi, and the gain variation is less than 1.65 dB. The measured average gain for the primary signal of type2, is approximately -2.05 dBi to -0.34 dBi with the gain variation of 1.71 dB. For the secondary antenna, the average gain is from -1.81 dBi to -0.16 dBi, and the gain variation is less than 1.65 dB. The antenna efficiency over the operating bandwidth of type1 is more useful for handheld mobile devices.

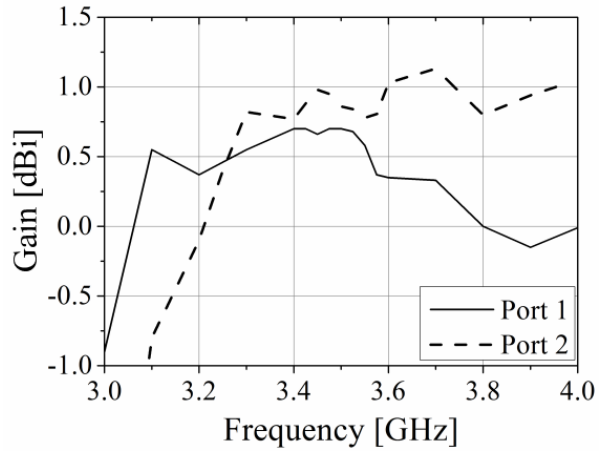

(a)

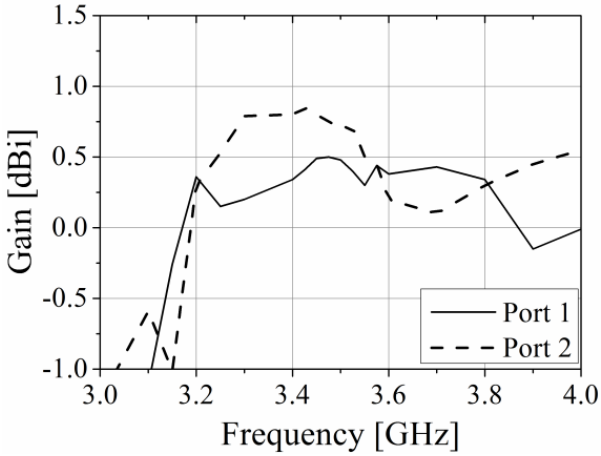

(b)

Fig. 6. Measured average gain, a) Type 1: Dual-port antenna based on CCSL antenna, (b) Type 2: Dual-port antenna based on polarization diversity.

Under the assumption of uniformly scattered radio environments, envelope correlation coefficient (ECC) between two antennas by using measured far field radiation patterns can be easily obtained from equation (1) [14].

$$\rho_{12} = \frac{\left|\oint\{(\mathrm{XPR}\cdot \mathrm{E}_{\theta MA}(\Omega)\cdot \mathrm{E}^{*}_{\theta SA}(\Omega) + \mathrm{E}_{\emptyset MA}(\Omega)\cdot \mathrm{E}^{*}_{\emptyset SA}(\Omega)\}\mathrm{d}\Omega\right|^{2}}{\oint\{\mathrm{XPR}\cdot \mathrm{G}_{\theta MA}(\Omega)+\mathrm{G}_{\emptyset MA}(\Omega)\}\mathrm{d}\Omega\cdot\oint\{\mathrm{XPR}\cdot \mathrm{G}_{\theta SA}(\Omega)+\mathrm{G}_{\emptyset SA}(\Omega)\}\mathrm{d}\Omega} \quad (1)$$

$E_{\theta MA}(\Omega)$ is the vertical polarization complex radiation pattern from the main antenna, $E_{\theta SA}(\Omega)$ is the vertical polarization complex radiation pattern from the sub-antenna, $E_{\emptyset MA}(\Omega)$ is the horizontal polarization complex radiation pattern from the main antenna, and $E_{\emptyset SA}(\Omega)$ is the horizontal polarization complex radiation pattern from the sub-antenna. Ω is the solid angle for a spherical coordinate system. When XPR = 1, the test environment is isotropic.

Fig. 7 shows ECC for the two types of antennas measured over the operating frequency range. Note that the ECC for both types of antennas are in acceptable range however, type 2 shows a slight increase of ECC near 3.4 GHz.

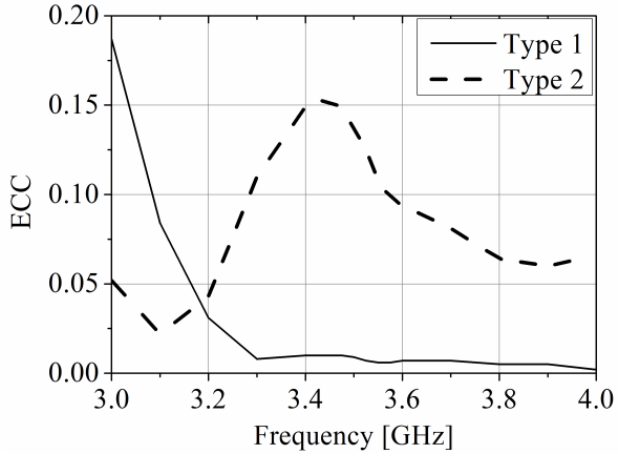

Fig. 7. Measured ECC characteristics.

Fig. 8 shows the measured 2-D radiation patterns in Azmith plane for co-polarization (Co-pol) and cross-polarization (X-pol) gain components of the two types of antennas. Port 1 for the both of antennas has strong directivities on X-pol gains and this creates pattern diversity between port 1 and port 2 for both of antennas. It is noted that the peaks at the X-pol gain of type 1 are at 115° and 255° resulting in smaller X-pol gain in the broad side of the antenna. This could be the reason for smaller ECC and better isolation characteristics observed on type 1 antenna.

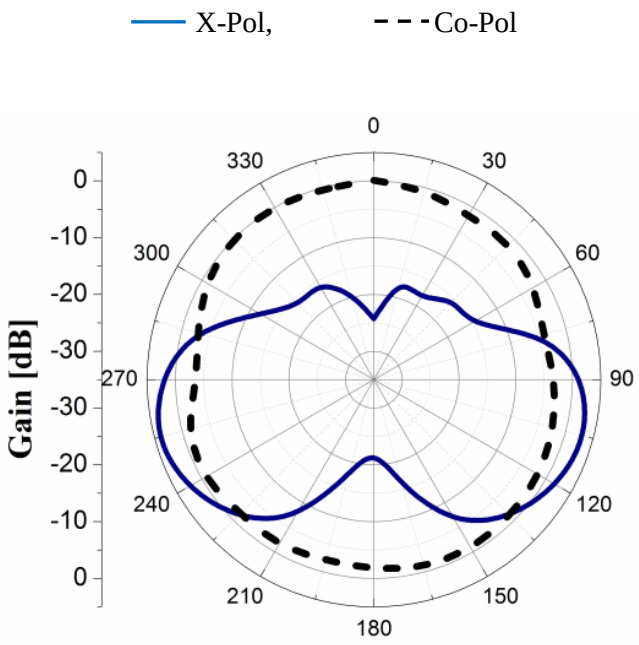
X-Pol,
Co-Pol
Gain [dB]
0
30
60
90
120
150
180
210
240
270
300
330
0
-10
-20
-30
-30
-20
-10
0

(a)

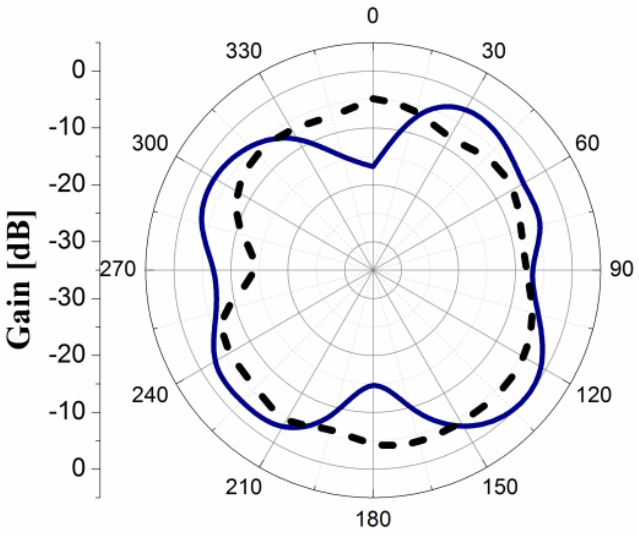
Gain [dB]
0
30
60
90
120
150
180
210
240
270
300
330
0
-10
-20
-30
-30
-20
-10
0

(b)

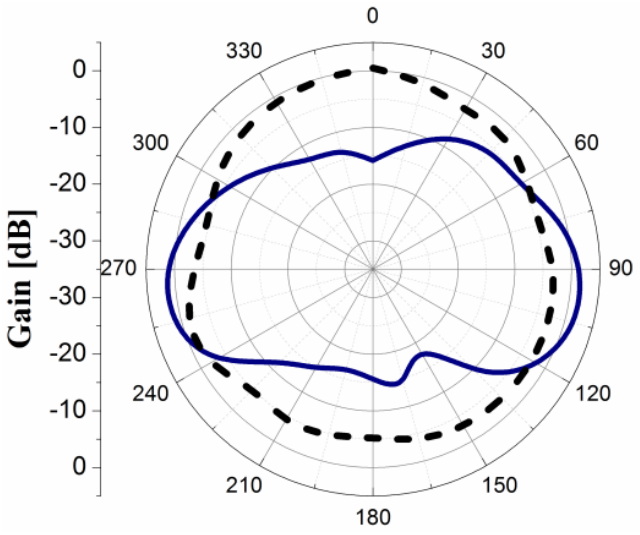

(c)

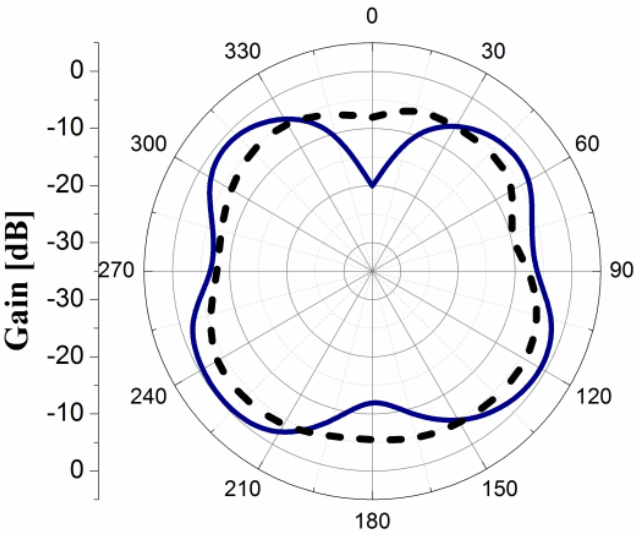

(d)

Fig. 8. The measured 2-D radiation patterns in Azmith plane at 3.5 GHz, (a) Port 1 of type 1, (b) Port 2 of type 1, (c) Port 1 of type 2, (d) Port 2 of type 2.

5. Conclusion

In this letter, a more size efficient, high isolation dual-port antenna design is proposed by merging IFA and a cross coupled semi-loop (CCSL) antenna. It is demonstrated that the proposed antenna shows greater port to port isolation performance compared with the polarization diversity based dual-port antenna through simulations and measurements. It is confirmed that the CCSL is helpful not only for improving the isolation characteristics but also

for wider operating bandwidth. Through this study, it is verified that the proposed dual-port antenna can be a promising antenna solution for the next generation mobile broadband standard which requires greater number of frequency band support and higher order MIMO under 6 GHz frequency ranges.

Acknowledgements

This work was supported by the research fund of Hanyang University (HY-2016).

References

[1] G. Ajay, L. Cheng-Jung, A. Maha, "Compact metamaterial quad-band antenna for mobile application," in *Proc. of IEEE Antennas and Propagation Society International Symposium*, pp. 1-4, July 2008. Article (CrossRef Link)
[2] R. Valkonen, J. Ilvonen, C. Icheln, P. Vainikainen, "Inherently non-resonant multi-band mobile terminal antenna," *Electronics Letters*, vol. 46, pp. 11-13, Jan. 2013. Article (CrossRef Link)
[3] [Online]. Available: Article (CrossRef Link)
[4] [Online]. Available: Article (CrossRef Link)
[5] A. Jain, P. K. Verma, V. K. Singh, "Performance analysis of PIFA based 4 x 4 MIMO antenna," *Electronics Letters*, vol. 48, pp. 474-475, Apr. 2012. Article (CrossRef Link)
[6] H. Dajung, L. Changhyeong, P. Heejun, K. Sungtek, "Antenna design for 4-by-4 MIMO communication," in *Proc. of International Conference on Signal Processing and Communication (ICSC)*, pp. 61-63, Dec. 2016. Article (CrossRef Link)
[7] H. T. Chattha, S.J. Boyes, Y. Huang, "Polarization and Pattern Diversity-Based Dual-Feed Plannar Inverted-F Antenna," *IEEE Trans. Antennas Propag.*, Vol. 60, No. 3, pp. 1532-1539, March 2012. Article (CrossRef Link)
[8] H. T. Chattha, M. Nasir, Q. H. Abbasi, Y. Huang, S.S. Alja'afreh, "Compact Low-Profile Dual-Port Wideband Plannar Inverted-F MIMO Antenna, " *IEEE Antennas Propag. Lett.*, Vol. 12, pp. 1673-1675, 2013. Article (CrossRef Link)
[9] Q. Rao, D. Wang, "A Comact Dual-Port Diversity Antenna for Long-Term Evolution Handheld Devices", *IEEE Trans. Veh Technol*., Vol. 59, No. 3, pp. 1319-1329. March 2010. Article (CrossRef Link)
[10] P. Bahramzy, O. Jagielski, Gerf F. Pedersen, "Thermal Loss and Soldering Effect Study of High-Q Antennas in Handheld Devices," in *Proc. of 7th EuCAP'2013*, pp. 878-881, 2013.
[11] Computer Simulation Technology (CST) Microwave Studio Suite 2014 [Online]. Available: Article (CrossRef Link).
[12] H. Hui, L. Buon Kiong, Y. Zhinong, H. Sailing, "Decoupling of Multiple Antennas in Terminals With Chassis Excitation Using Polarization Diversity, Angle Diversity and Current Control," *IEEE Trans. Antennas Propag.*, Vol. 60, No. 12, pp. 5947-5957, Dec. 2012. Article (CrossRef Link)
[13] Microwave Technologies Group [Online]. Available: Article (CrossRef Link)
[14] I. Szimi, G. F. Pedersen, S. C. Del Barrio, M. D. Foegelle., "LTE Radiated Data Throughput Measurements, Adopting MIMO 2x2 Reference Antennas," in *Proc. of IEEE Vehicular Technology Conference*, pp. 1-5, Fall, 2012. Article (CrossRef Link)

Hyung-kyu Yang received the B.S. degree in Electronics engineering from Chungnam National University, Korea, in 1989, and the M.S. degree in Electrical & Computer Engineering from Hanyang University, in 2000. He is currently working as a professor in Department of Information & Communication System, Korea Polytechnics College. His research interest includes the area of design and analysis of Network system, NGN, Wireless communication.

Won-Woo Lee received the B.S. degree in Electronics and Physics from Kwangwoon University, Korea, in 2000, and the M.S. degree in microwave engineering from Kwangwoon University, in 2002, and the Ph.D. degree in Electrical and Computer Engineering from Hanyang University, in 2014. He is currently working as a research engineer at Korea Expressway Corporation. His research interest includes the area of design and analysis of LTE system, 5G mmWave system, antenna and microwave circuit design.

Byung-Ho Rhee received the B.S. and M.S. degrees in electronics engineering from Hanyang University, Seoul, Korea in 1975 and 1977, respectively, and the Ph.D. degree in electric and electronics engineering from National Chiba University, Chiba, Japan in 1993. Since 1981, he has been a Professor in the College of Information and Communications at Hanyang University, Seoul, Korea. From 2006 to 2008, he was the Dean of the college. His primary research interests include network management, software defined radio, MIMO System, NGN, and security in wireless network.